Supplement of The Cryosphere, 12, 1–24, 2018
https://doi.org/10.5194/tc-12-1-2018-supplement

The Cryosphere
Open Access

Supplement of

Future snowfall in the Alps: projections based on the EURO-CORDEX regional climate models

P. Frei et al.

Correspondence to: Sven Kotlarski (sven.kotlarski@meteoswiss.ch)

Supplementary Material, Part A
General Analysis

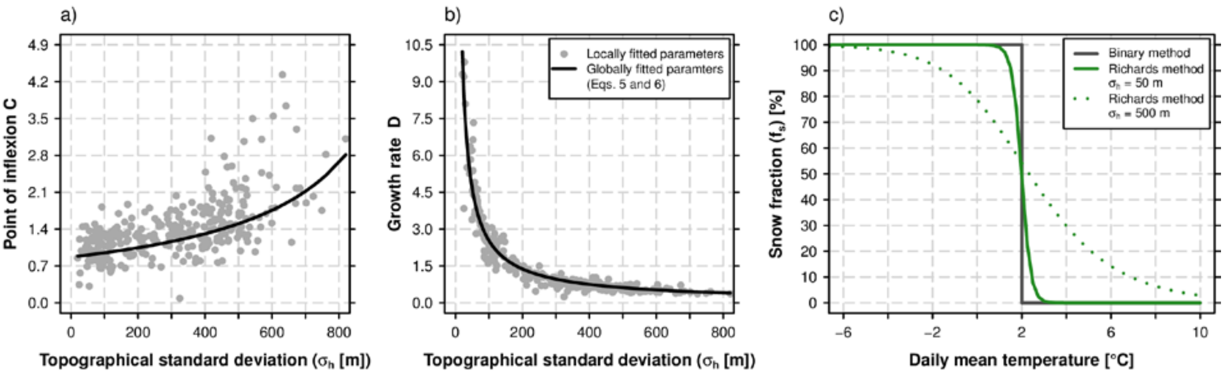

Figure S1 a) and b) Expressing the point of inflexion C and the growth rate D of the Richards equation as a function of the subgrid topographical standard deviation. Grey circles: Fitted parameters for each grid cell in the Swiss domain. Black line: Global fit. c) Example for deriving the daily snow fraction *sf* based on the binary method with a snow fractionation temperature T^*=2°C (gray line) and based on the Richards method assuming subgrid topographical standard deviations of 50 m (solid green line) and 500 m (dotted green line).

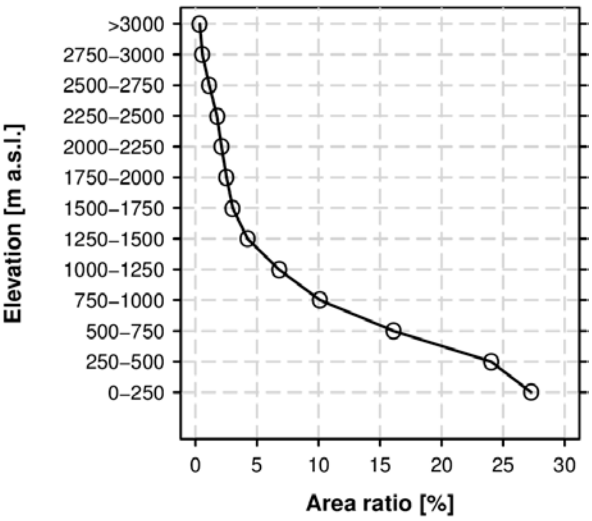

Figure S2 Elevation-area distribution of the Alpine analysis domain (see Fig. 1 of the main manuscript) based on the high-resolution GTOPO30 digital elevation model (https://lta.cr.usgs.gov/GTOPO30) aggregated to a regular grid of 1.25 arc seconds (about 2 km). The area ratio provides the percentage contribution of a given elevation interval to the total area assuming equal grid cell areas.

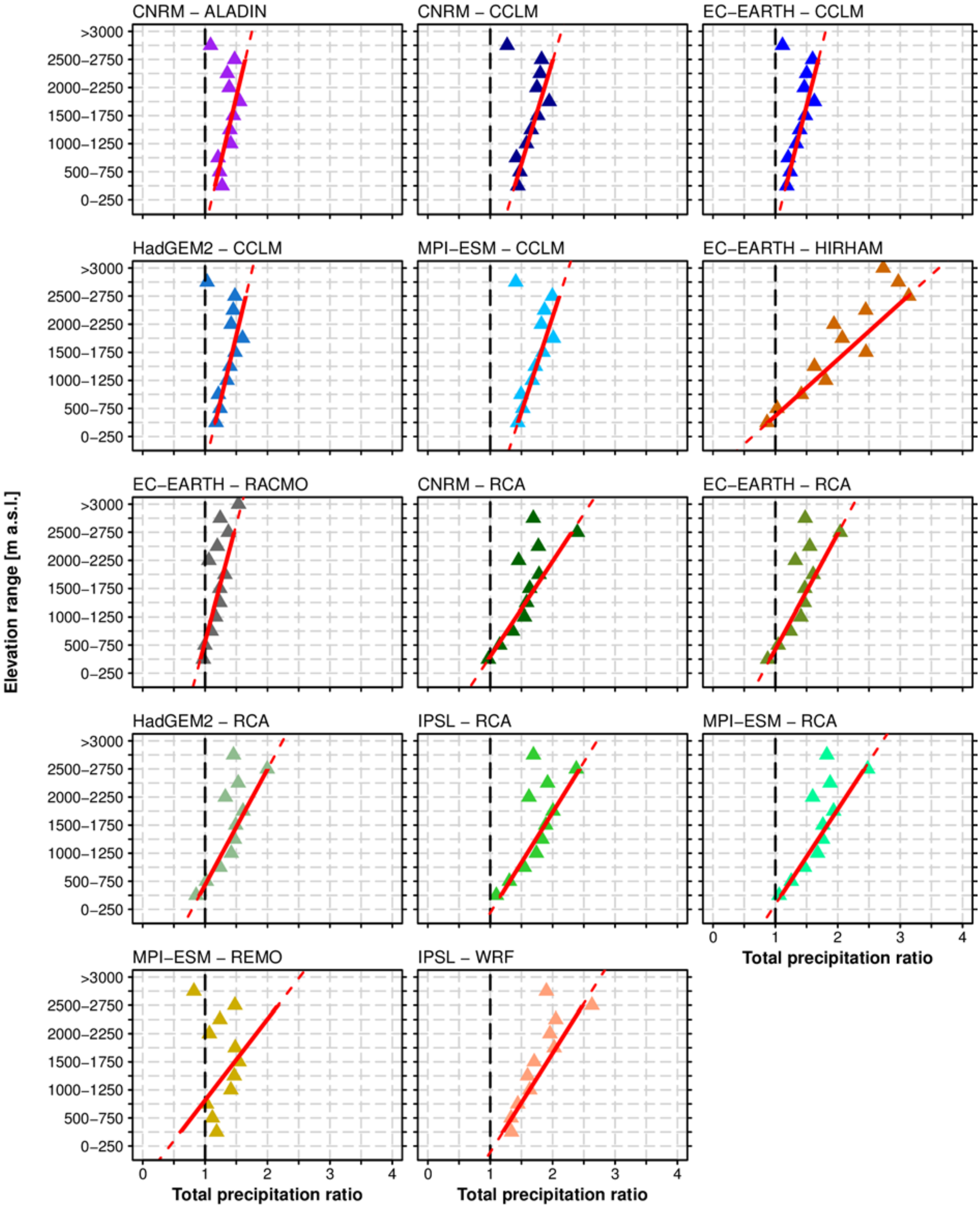

Figure S3: Ratios (RCM simulations of the full model set divided by observational analysis) of total precipitation sums from September to May in 1971 - 2005 vs. elevation for the Swiss domain. The linear regression line, applied to the ratios for elevations between 250 m a.s.l. and 2750 m a.s.l., is represented by the red line.

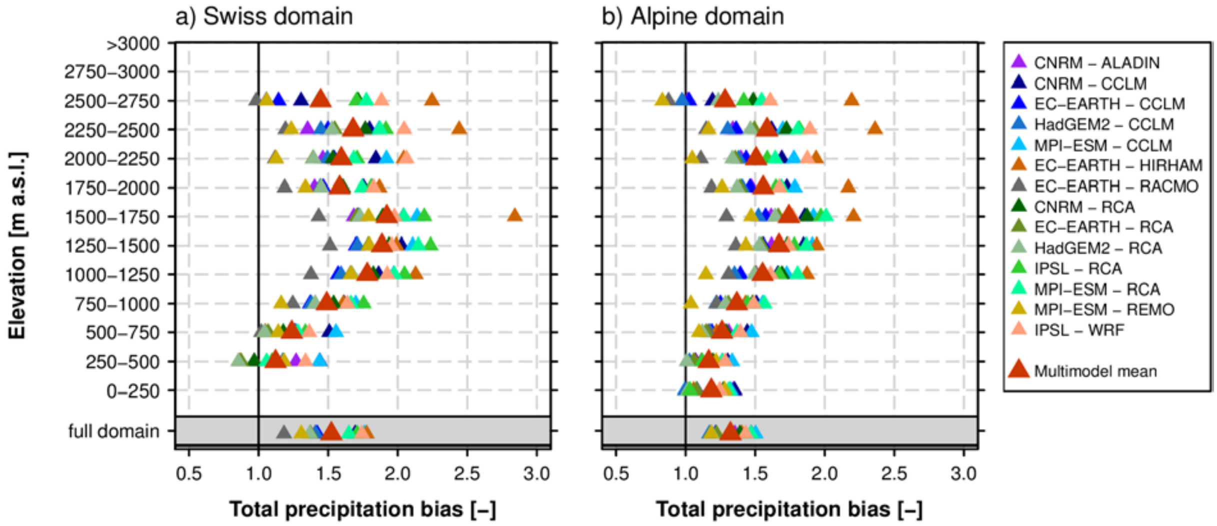

Figure S4: Total winter (SEP-MAY) precipitation bias (expressed as quotient between RCM simulations of the full model set and observations) in the EVAL period 1971-2005 for individual elevation intervals and for the full domain (lowermost row). Left panel: Swiss domain only. Right panel: Entire Alpine analysis domain (cf. Fig. 1). Observational reference: EOBS version 13.1 (Haylock et al., 2008) on 0.22° interpolated to the 0.11° RCM grid by nearest neighbour interpolation.

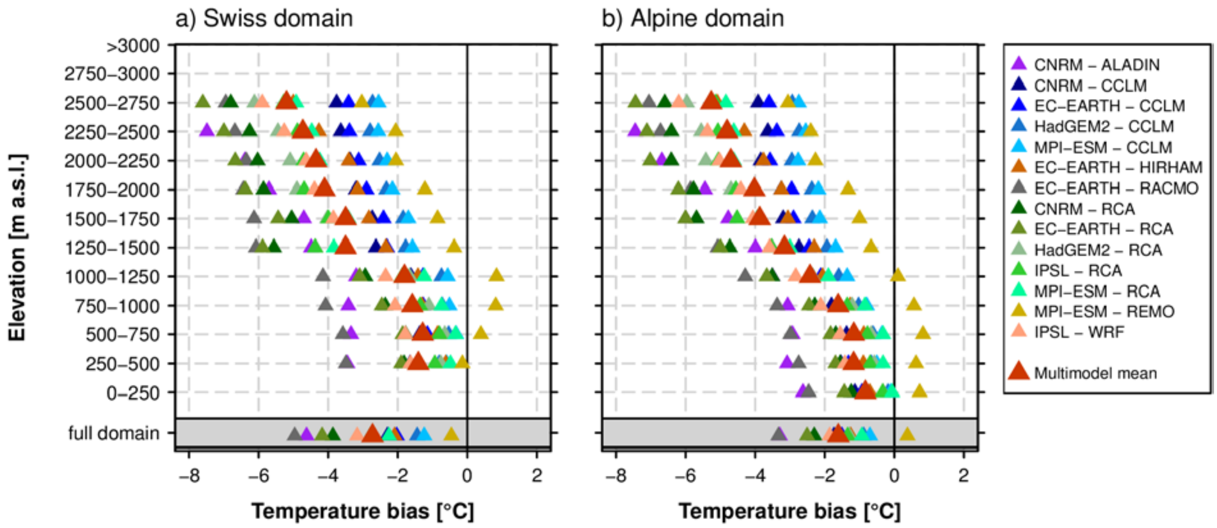

Figure S5: As Figure S4 but for the winter (SEP-MAY) temperature bias.

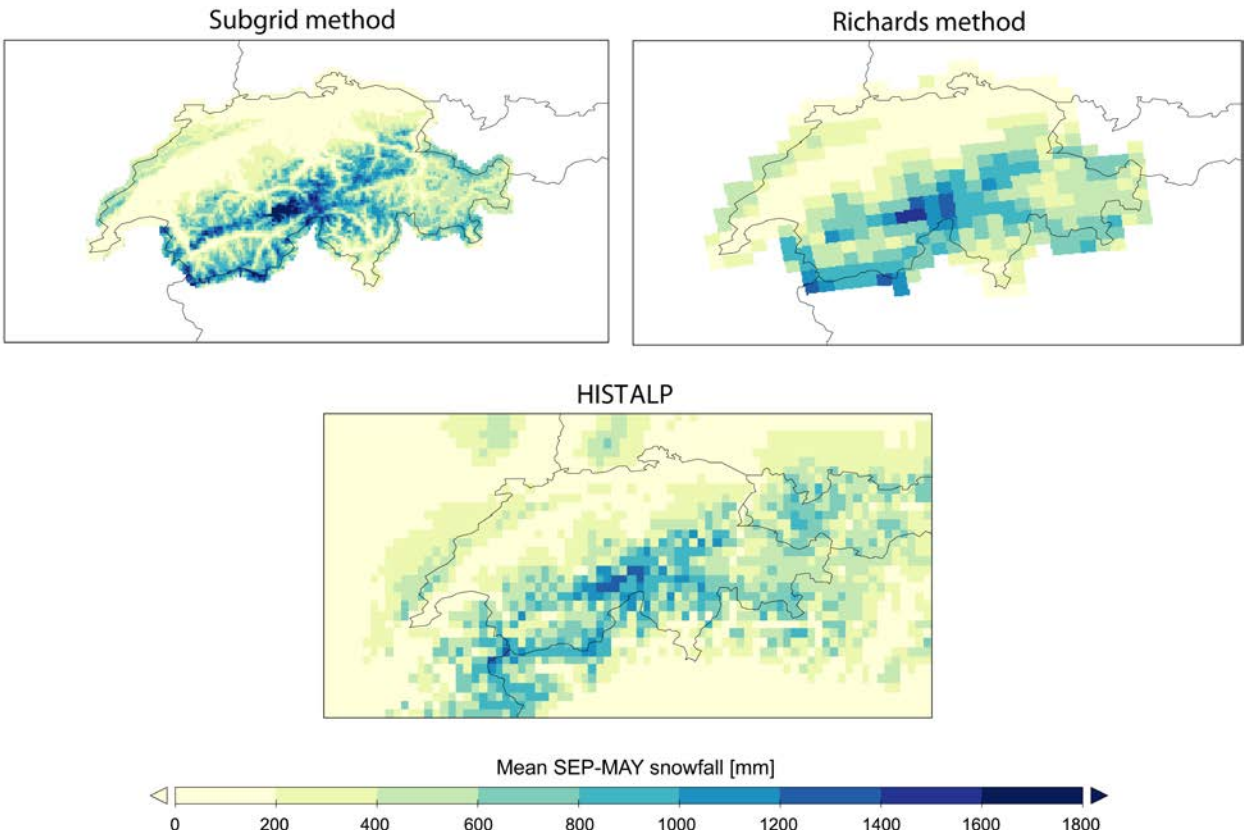

Figure S6 Mean September-May snowfall sum [mm] in the period 1971-2005 as represented by the 2 km snowfall reference (subgrid method; upper left), the 12 km snowfall reference on the RCM grid (Richards method; upper right) and the HISTALP dataset (Chimani et al., 2011; lower).

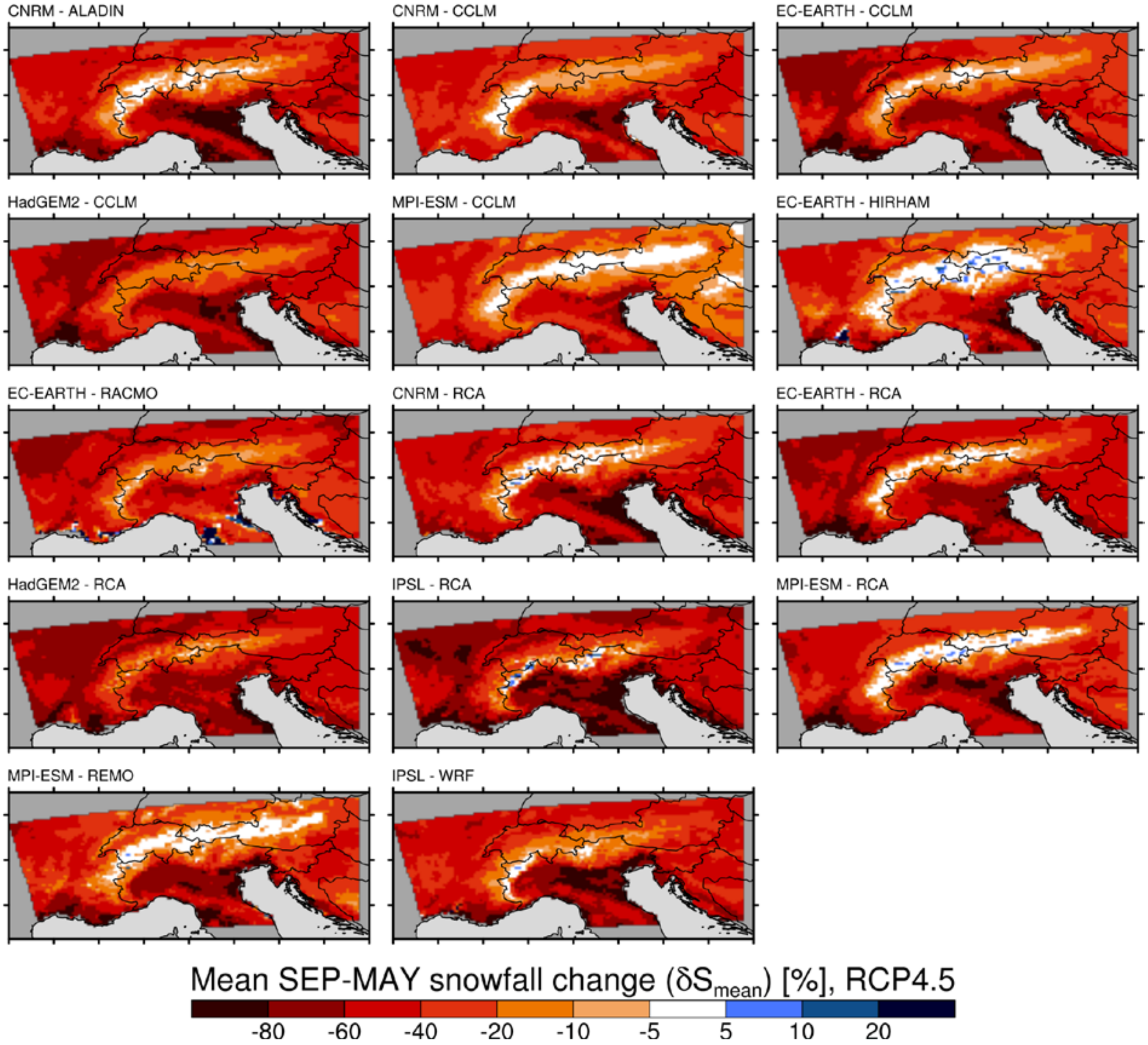

Figure S7 Spatial distribution of relative changes (SCEN period 2070-2099 with respect to CTRL period 1981-2010) in mean September-May snowfall, δS_{mean}, for RCP4.5 and for the 14 snowfall separated–bias-adjusted RCM simulations (RCM_{sep+ba}) of the full model set.

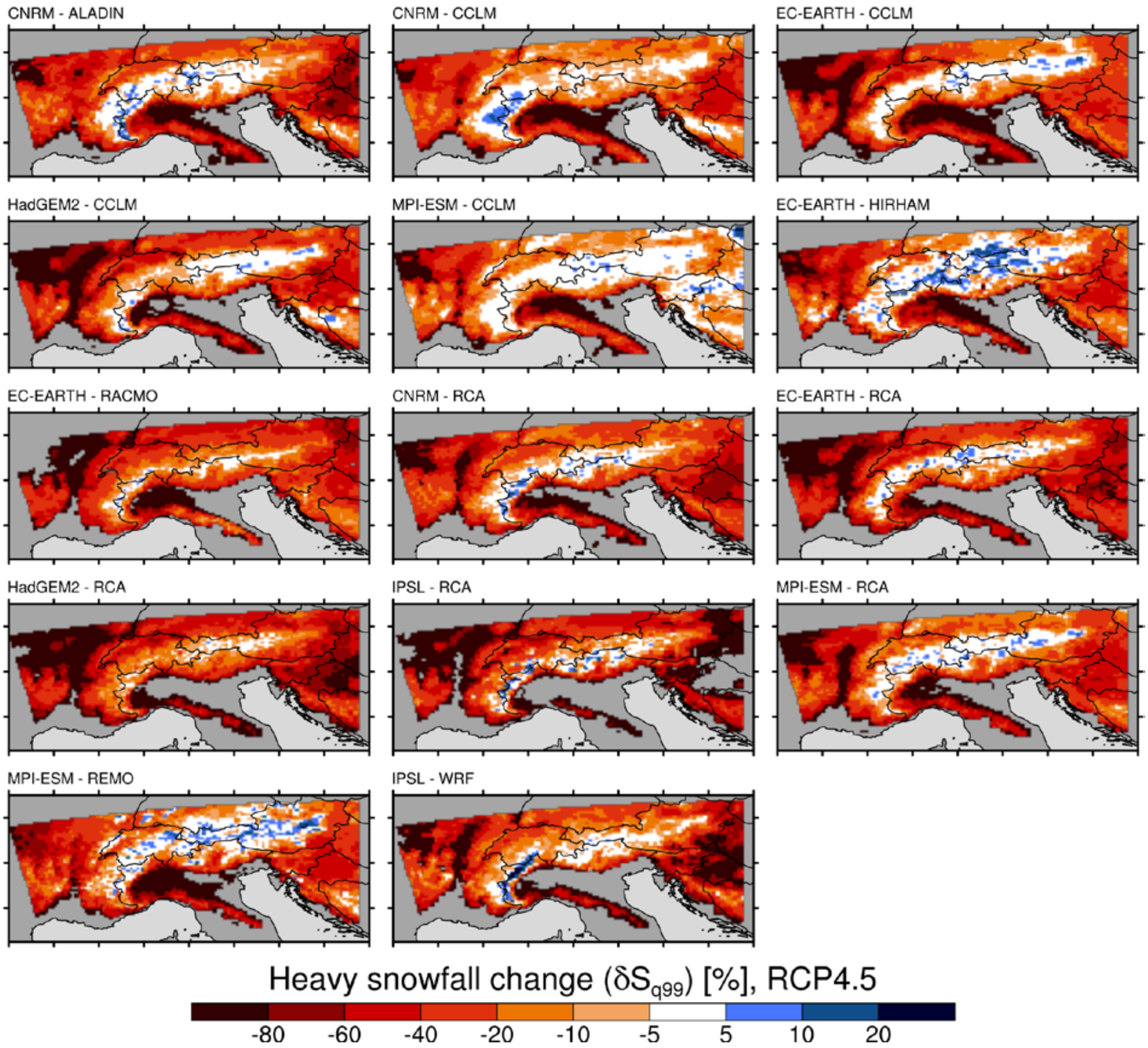

Figure S8 Spatial distribution of relative changes (SCEN period 2070-2099 with respect to CTRL period 1981-2010) in heavy snowfall, δS_{q99}, for RCP4.5 and for the 14 snowfall separated–bias-adjusted RCM simulations (RCM_{sep+ba}) of the full model set.

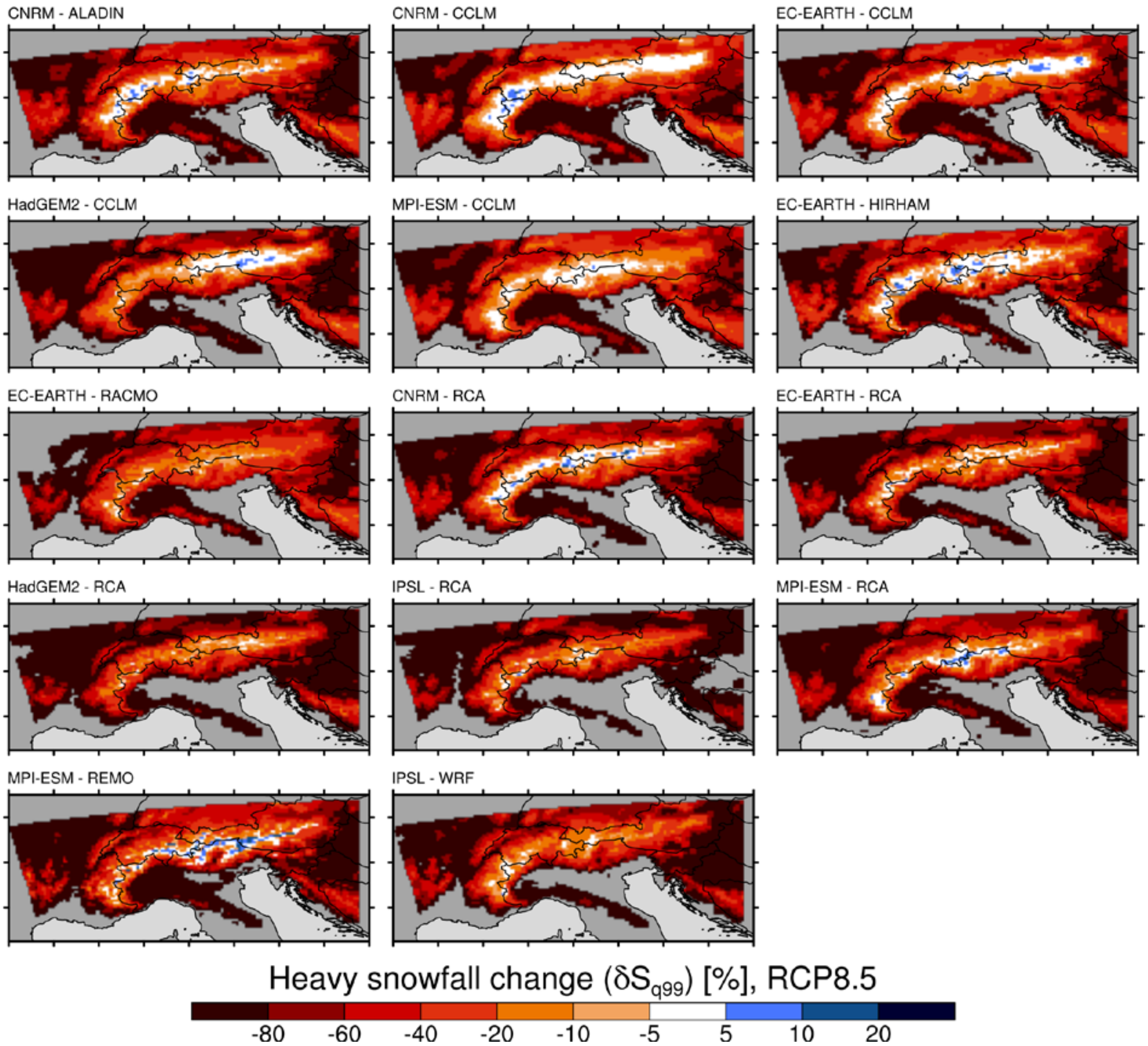

Figure S9 Spatial distribution of relative changes (SCEN period 2070-2099 with respect to CTRL period 1981-2010) in heavy snowfall, δS_{q99}, for RCP8.5 and for the 14 snowfall separated–bias-adjusted RCM simulations (RCM_{sep+ba}) of the full model set.

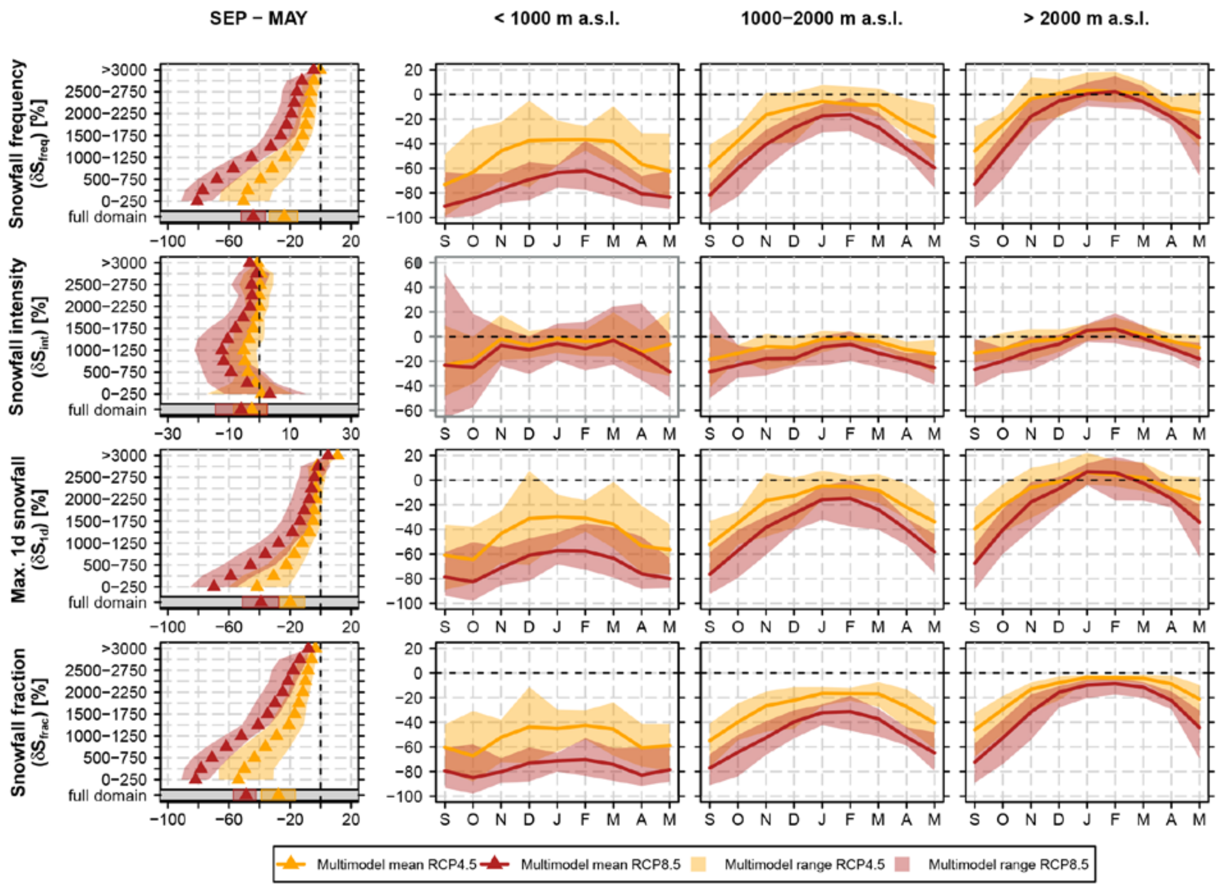

Figure S10 Relative changes (SCEN period 2070-2099 with respect to CTRL period 1981-2010) of max. 1 day snowfall, δS_{1d}, snowfall frequency, δS_{freq}, snowfall intensity, δS_{freq}, and snowfall fraction, δS_{frac}, based on the 12 snowfall separated–bias-adjusted (RCM_{sep+ba}) RCM simulations of the reduced model set for RCP4.5 and RCP8.5, each. The first column shows the mean September-May snowfall index statistics vs. elevation while monthly snowfall index changes (spatially averaged over the elevation intervals <1000 m.a.s.l., 1000 m a.s.l.-2000 m a.s.l. and >2000 m a.s.l.) are displayed in columns 2-4.

Supplementary Material, Part B
Climate Model Selection

Our analysis initially considered all EURO-CORDEX GCM-RCM combinations available in December 2016 that provide experiments for the higher EUR-11 resolution and for both RCP4.5 and RCP8.5. Out of this initial set individual combinations were either completely or partly removed from the analysis due to the reasons outlined below. The reduced model set consists of 12 GCM-RCM chains (see Table 1 of the main manuscript) and is consistent with the current model selection for the upcoming CH2018 Swiss Climate Scenarios (*www.ch2018.ch*). In the present work all ensemble-based analyses that do not allow an identification of individual experiments are carried out for this reduced set only. Fig. 12 of the main manuscript, however, is replicated for the full set which allows an intercomparison of the results for both selections (Fig. S15).

MPI-ESM-REMO

Two realisations of the GCM-RCM chain MPI-ESM-REMO are available (initial condition ensemble sampling internal climate variability). In order to avoid mixing GCM-RCM sampling with pure internal climate variability sampling, the second realisation of this model chain was removed and only the first one was considered.

HadGEM2-RACMO and EC-EARTH-RACMO

These two model chains are subject to a widespread continuous accumulation of snow cover at high alpine grid cells in the course of the 21st century. For individual grid cells several tens of meters of snow water equivalent are obtained. The extensive snow accumulation has obvious feedbacks on the climate change signal of 2m temperature: Temperature change signals are considerably lower at the affected grid cells than in surrounding regions. The summer season JJA, which is excluded from our analysis, is most affected (Fig. S11). But also neighbouring months are concerned (Fig. S12). The ultimate reason for this behaviour is not clear, but the issue is potentially critical for our analysis as 2m temperature change signals directly influence future snowfall changes via changes of the precipitation phase. HadGEM2-RACMO, which is subject to the highest spatial variability of temperature change signals in the May/September mean, has therefore been completely omitted in this study. EC-EARTH-RACMO is considered in the full but not in the reduced model set (see Table 1 of the main manuscript).

IPSL-WRF

This model chain is subject to suspicious precipitation and temperature change signals in the northern part of the Alps that at least partly have to be considered to be unphysical. The most affected season is summer (JJA), but also adjacent months are concerned. In detail, the RCM output in terms of precipitation along the northern flanks of the Alps shows a very low correlation with precipitation amounts in the driving GCM (Fig. S13) and an opposite future change signal (summer precipitation increase instead of a clear summer precipitation decrease in the driving GCM; Fig. S13). Furthermore, the simulated temperature evolution in summer (JJA) and partly also in autumn (SON) is subject to a sudden shift to lower levels around year 2023 (Fig. S14). This feature is not apparent in the driving GCM and cannot be explained on a physical basis. The IPSL-WRF model chain is therefore considered as part of the full model set, i.e. in places where identification of individual models is possible, but is not contained in the reduced model set (see Table 1 of the main manuscript).

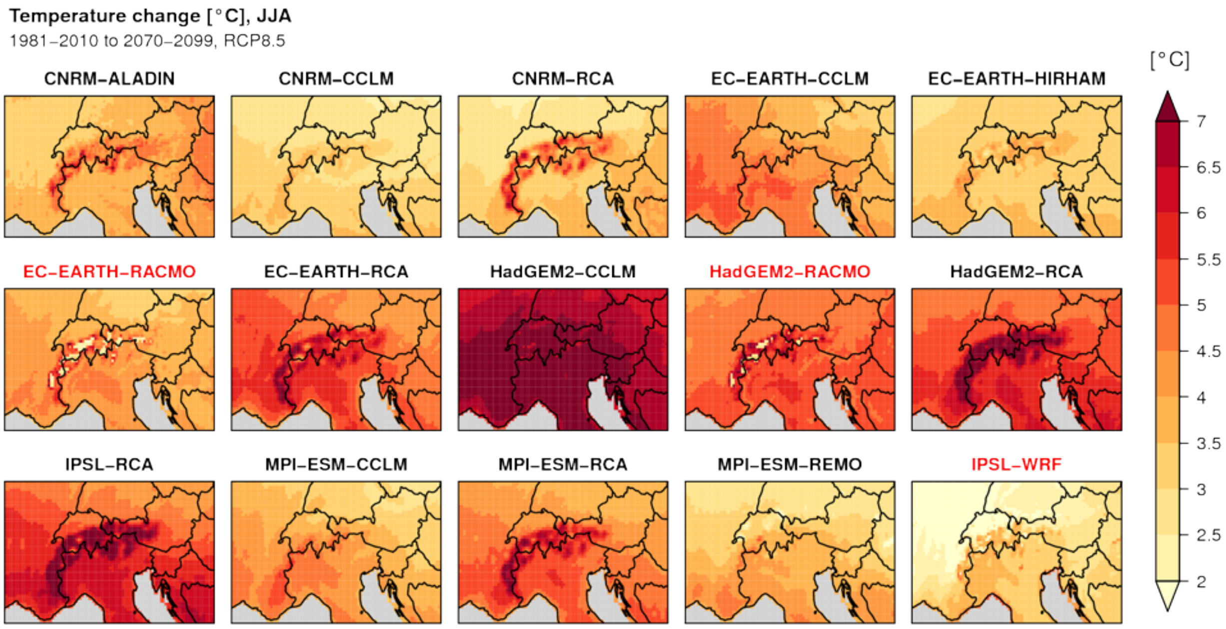

Figure S11 Spatial pattern of summer (JJA) temperature change signals (2070-2099 with respect to 1981-2010) for RCP8.5 in the 15 EUR-11 GCM-RCM model chains that were available in December 2016. Red font denotes models that were either completely or partly removed from our analysis. Note the considerable lower change signal over high-alpine grid cells in EC-EARTH-RACMO and HadGEM2-RACMO.

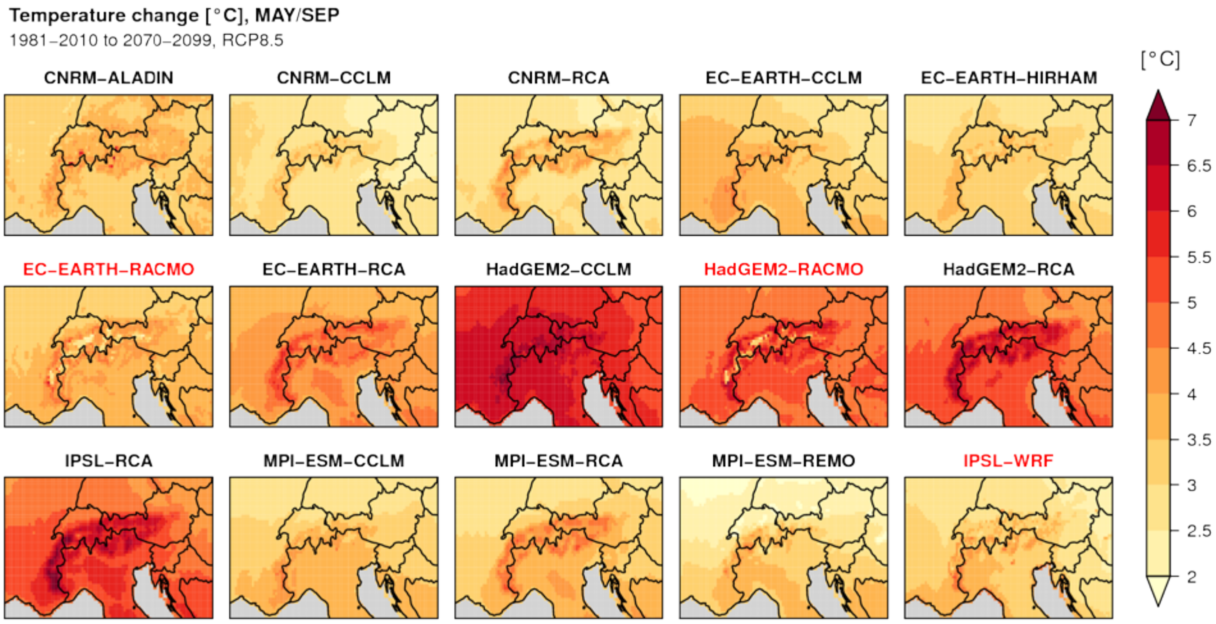

Figure S12 As Fig. S11 but for the mean May/September temperature change signal.

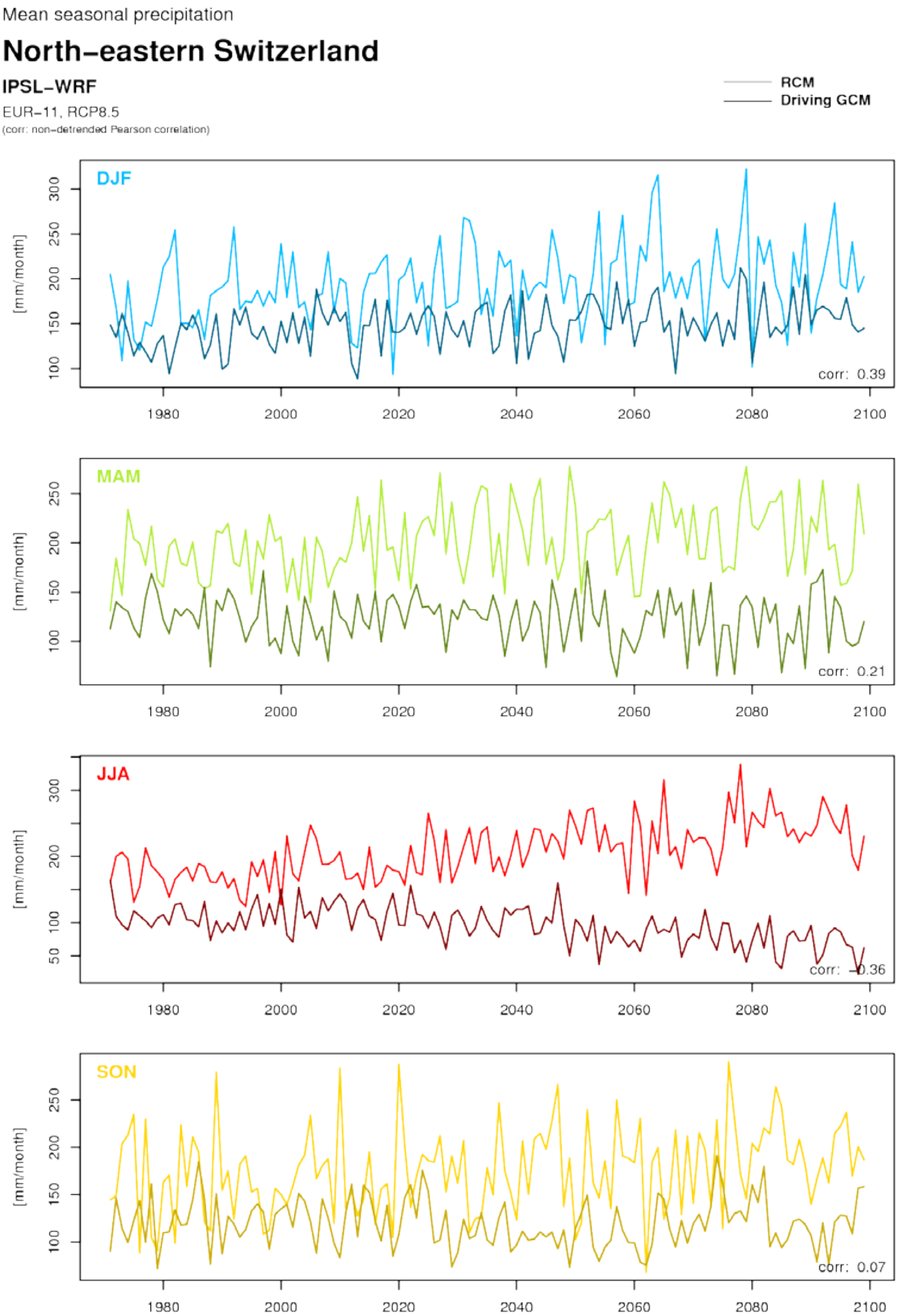

Figure S13 Evolution of seasonal mean precipitation over north-eastern Switzerland in EUR-11 IPSL-WRF for RCP8.5. Dark line: driving GCM (IPSL), bright line: RCM (WRF). The number in the lower right corner of each panel indicates the non-detrended Pearson correlation coefficient of mean seasonal precipitation in the RCM and its driving GCM. Note the negative correlation in summer (JJA) and the opposing summer precipitation trends.

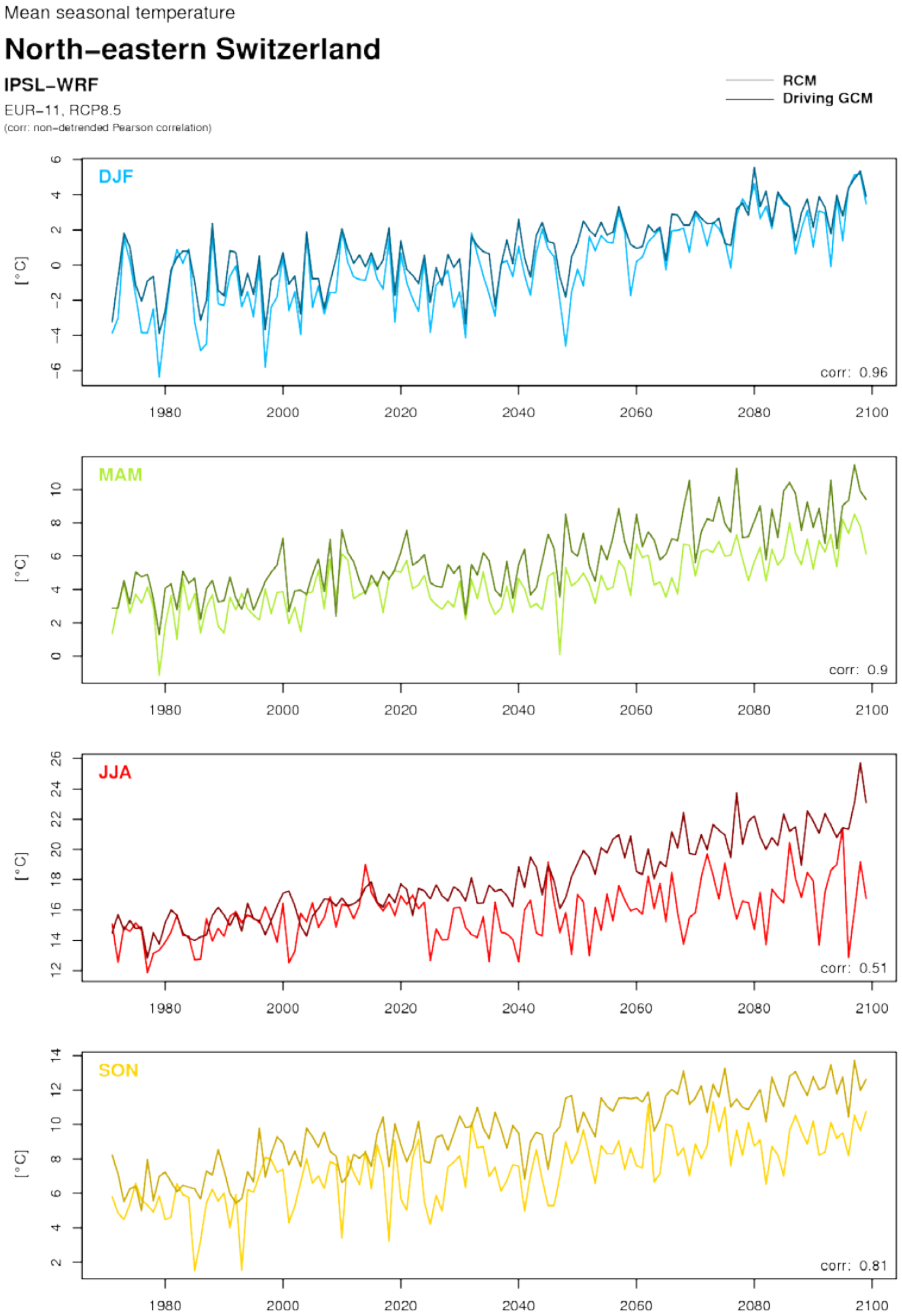

Figure S14 As Fig. S13 but for seasonal mean temperature. Note the low correlations of summer (JJA) temperatures and the apparent shift of summer (JJA) and autumn (SON) temperatures in the RCM around year 2023.

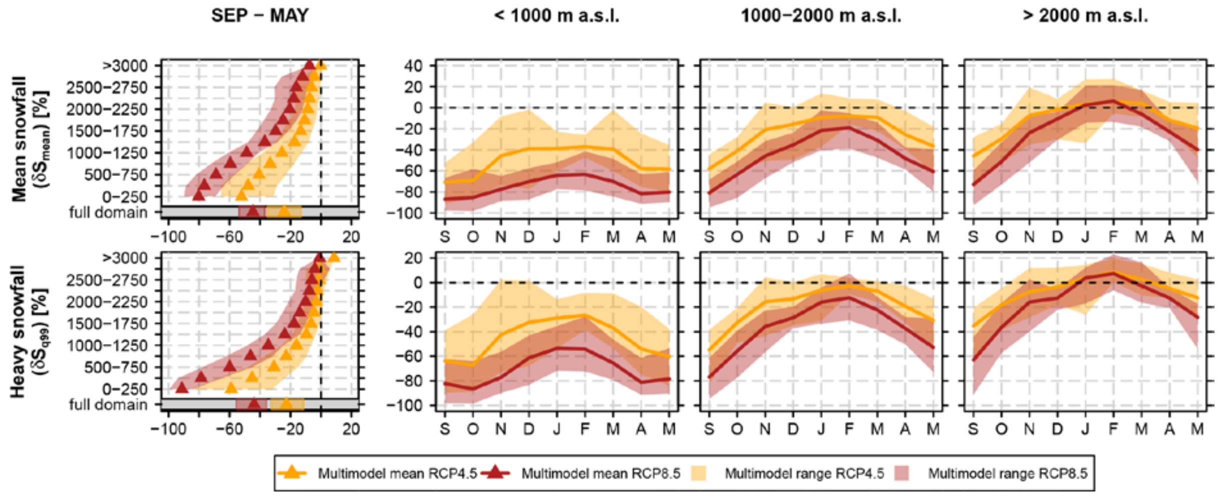

Figure S15 As Fig. 12 of the main manuscript but for the full model set (14 RCM simulations for each emission scenario).